Astron. Astrophys. 163, 119–134 (1986)

ASTRONOMY
AND
ASTROPHYSICS

B[e]-supergiants of the Magellanic Clouds*

F.-J. Zickgraf[1], B. Wolf[1], O. Stahl[2], C. Leitherer[1], and I. Appenzeller[1]

[1] Landessternwarte, Königstuhl, D-6900 Heidelberg 1, Federal Republic of Germany
[2] ESO, Karl-Schwarzschild-Str. 2, D-8046 Garching bei München, Federal Republic of Germany

Received October 18, accepted November 13, 1985

Summary. Spectroscopic and photometric observations at the satellite UV, visual, and infrared wavelengths of 8 Magellanic Clouds dusty B[e]-supergiants (R 4, R 50, R 66, R 82, R 126, Hen S 12, Hen S 22, and Hen S 134) are discussed. In spite of their high luminosity these stars show little or no photometric or spectroscopic variations. Apart from R 66 (B8Ia) all stars are early B supergiants (B0–B3). The peculiar emission line spectra appear to be a consequence of unique wind characteristics. A two component stellar wind model, comprising a slow, dense, cool equatorial wind and a normal radiation driven wind in the polar region, can account for the observations. We conclude that the known B[e]-stars of the Magellanic Clouds are massive ($30 \lesssim M \lesssim 80\,M_\odot$) post-main-sequence objects where stellar rotation plays an important role for the mass loss.

Key words: magellanic clouds – early-type stars – emission line – supergiants – circumstellar matter

1. Introduction

The early-type supergiant stars in the Magellanic Clouds (MCs) include a class of objects, the B[e]-stars, which are characterized by the following typical properties: a) strong Balmer emission lines, frequently with P Cygni profiles, b) permitted and forbidden emission lines of Fe II, [Fe II], [O I] etc., c) strong infrared excess due to thermal radiation of circumstellar dust. At present eight B[e]-stars are known in the MCs: R 4 and R 50 of the SMC, R 66, R 82, R 126, Hen S 12, Hen S 22, Hen S 134 of the LMC. The peculiar character of the line spectra in the visual range was known since long (e.g. Cannon, 1924; Henize, 1956; Smith, 1957; Feast et al., 1960), whereas their IR excess was discovered only a few years ago (Allen and Glass, 1976; Glass, 1977; Stahl et al., 1983; Stahl et al., 1984). The B[e]-supergiants of the Magellanic Clouds belong to the most luminous and presumably most massive stars in these galaxies. Despite some common spectroscopic features the B[e]-stars differ profoundly from the other hot luminous stars in the Clouds. Unlike the S Dor variables e.g. they appear rather stable both photometrically and spectroscopically. The question whether different or additional mechanisms may drive the mass loss in these stars is of particular interest in connection with current theories of stellar evolution and stellar stability in the upper part of the HR-diagram. Our group has previously studied two of the B[e]-supergiants in the LMC. For R 66 Stahl et al. (1983) assumed a spherically symmetric model with a gravitationally decelerated stellar wind originating from a B8Ia supergiant. In the case of R 126 Zickgraf et al. (1985) (hereafter referred to as Paper I) suggested a non-spherical two-component wind model with a disk-like outer configuration. The disk is supposed to be formed by a rotation-enhanced slow, cool and dense wind. In the polar region a normal high velocity line-driven wind of an early-type supergiant is assumed. In the present paper we shall show that this model can be extended to *all* MC B[e]-supergiants.

2. Observations

2.1. Photometry

In order to study the photometric properties of the programme stars we combined published results by Smith (1957), Feast et al. (1960), Westerlund (1961), Westerlund et al. (1963), Basinski et al. (1967), Mendoza (1970), Butler (1972), Ardeberg et al. (1972), Dachs (1972), Appenzeller (1972), Osmer (1973), Azzopardi and Vigneau (1975), Ardeberg and Maurice (1977), Isserstedt (1978), Isserstedt (1979) with our own *UBV(RI)*-observations carried out during several observing runs between 1980 and 1984. Our measurements were obtained at the ESO 50 cm telescope, partly in the Johnson *UBV*-system with an EMI 6256 multiplier and partly using *UBVRI*-filters (Bessell, 1979) with an RCA 31034 A (Quantacon) photomultiplier. Usually a 15″ diaphragm was used. The data for R 4, R 50, R 82, S 12, S 22, and S 134 are summarized in Table 1a–f. The corresponding data for R 66 and R 126 were summarized in Stahl et al. (1983) and Paper I, respectively. In addition R 50 has been measured in the Strömgren-*uvby* system during five nights between Sept. 1 and 9, 1983 at the ESO 50 cm telescope equipped with an EMI 6256 photomultiplier. R 66 has been monitored differentially within the "long-term photometry of variables" – programme (Sterken, 1983) in the *uvby* system. These observations were carried out at ESO, La Silla, between October 1982 and December 1983 within 6 observing runs using the Bochum 61 cm and ESO 50 cm telescope with a single channel

Send offprint requests to: F.-J. Zickgraf

* Based on observations collected at the European Southern Observatory at La Silla, Chile and on data from the International Ultraviolet Explorer received from the Villafranca Data Archive of the European Space Agency

Table 1. Visual photometry obtained with broad-band filters

	System	V	$B-V$	$U-B$	$V-R$	$V-I$
a) R 4						
Basinski, Bok, Bok (1967)	*UBV*[a]	13.05	0.17	−0.80	–	–
Butler (1972)	*UBV*	13.15	0.09	−0.63	–	–
Osmer (1973)	*V*	13.02	–	–	–	–
Azzopardi, Vigneau (1975)	*UBV*	13.19	0.07	−0.83	–	–
Ardeberg, Maurice (1977)	*UBV*	13.11	0.12	−0.78	–	–
August 1983	*UBVRI*	13.06	0.13	−0.72	0.42	0.51
August 1984	*UBV*	13.02	0.15	−0.76	–	–
b) R 50						
Feast et al. (1960)	*BV*	11.56	0.19	–	–	–
Westerlund et al. (1963)	*UBV*	11.55	0.17	−0.39	–	–
Ardeberg, Maurice (1977)	*UBV*	11.57	0.17	−0.35	–	–
Isserstedt (1978)	*UBV*	11.57	0.18	−0.33	–	–
December 1981	*UBV*	11.55	0.19	−0.37	–	–
August 1983	*UBVRI*	11.56	0.19	−0.37	0.33	0.46
c) R 82						
Smith (1957)	*V*	12.05	–	–	–	–
Mendoza (1970)	*BVRI*	11.88	0.06	–	0.43	0.36
Ardeberg et al. (1972)	*UBV*	11.88	0.05	−0.66	–	–
Dec. 1981/Jan. 1982	*UBV*	11.98	0.03	−0.66	–	–
February 1983	*UBV*	11.98	0.03	−0.66	–	–
August 1983	*UBVRI*	11.93	0.06	−0.64	0.26	0.31
January 1984	*UBV*	12.00	0.02	−0.67	–	–
April 1984	*UBVRI*	11.94	0.07	−0.68	0.26	0.31
August 1984	*UBV*	12.03	0.03	−0.59	–	–
Dec. 1984	*UBVRI*	11.92	0.04	−0.66	0.24	0.30
d) Hen S 12						
Ardeberg et al. (1972)	*UBV*	12.68	0.05	−0.68	–	–
Isserstedt (1979)	*UBV*	12.56	0.08	−0.74	–	–
August 1983	*UBV*	12.68	0.05	−0.68	–	–
August 1984	*UBV*	12.59	0.07	−0.75	–	–
Dec. 1984	*UBVRI*	12.59	0.10	−0.70	0.29	0.39
e) Hen S 22						
Smith (1957)	*V*	11.85	–	–	–	–
Dachs (1972)	*UBV*	11.75	0.27	−0.72	–	–
Ardeberg et al. (1972)	*UBV*	11.83	0.19	−0.70	–	–
February 1980	*UBV*	11.74	0.28	−0.72	–	–
Dec. 1981/Jan. 1982	*UBV*	11.74	0.28	−0.68	–	–
February 1983	*UBV*	11.78	0.28	−0.68	–	–
August 1983	*UBVRI*	11.72	0.30	−0.69	0.96	0.76
January 1984	*UBV*	11.76	0.25	−0.61	–	–
April 1984	*UBVRI*	11.77	0.29	−0.66	0.94	0.73
August 1984	*UBV*	11.79	0.23	−0.62	–	–
Dec. 1984	*UBVRI*	11.77	0.27	−0.60	0.93	0.72
f) Hen S 134						
Westerlund (1961)	*BVRI*	12.07	0.22	–	1.81	1.04
Ardeberg et al. (1972)	*UBV*	12.06	0.27	−0.97	–	–
August 1983	*UBVRI*	11.89	0.43	−1.03	0.93	0.99
January 1984	*UBV*	12.03	0.25	−1.03	–	–
April 1984	*UBVRI*	11.83	0.46	−1.07	0.87	0.85
August 1984	*UBV*	12.03	0.29	−1.04	–	–
Dec. 1984	*UBVRI*	11.89	0.45	−1.00	0.87	0.86

[a] Photographic measurement

Table 2. Journal of *uvby*-observations of R 66 carried out within the "Long-term Photometry of Variables" (Sterken 1983)

Date of observing run	Number of observations	Observer
01.Oct.82–01.Nov.82	9	O. Stahl
01.Dec.82–21.Dec.82	1	M. de Groot
18.Jan.83–15.Feb.83	5	D. van der Linden
15.Aug.83–09.Sep.83	4	F.-J. Zickgraf
09.Sep.83–01.Oct.83	2	H. Ott
07.Dec.83–03.Jan.84	1	O. Stahl

photometer and an EMI 6256 photomultiplier. The technical data of these observations is given in Table 2.

In August 1983 *JHKLM*-photometry of all programme stars was done at ESO in La Silla, Chile, with the 1-m telescope equipped with a liquid nitrogen-cooled InSb detector. Technical details of these observations have been described by Stahl et al. (1984). R 66 had been observed in August 1982 already with the same equipment (cf. Stahl et al., 1983). For several objects the IR photometry was repeated in January 1984. However, in this run a different *L*-filter (with an effective wavelength of 3.8 μm instead of 3.6 μm) was used. (For a detailed description of the ESO filter system see Wamsteker, 1981). Table 3 summarizes the results of our IR observations and all corresponding published data (see Allen and Glass, 1976; Bensammar et al., 1983; Glass, 1977; Glass, 1984). Also included are the *N*-magnitudes published by Glass (1984).

Table 3. Infrared photometry of the B[e]-stars, AGL (1976) = Allen and Glass (1976), BEN (1983) = Bensammar et al. (1983). The numbers in brackets are the errors in 1/100 mag. The accuracy of our own measurements is <0.05 mag in *JHKL* and <0.20 in *M*, if not explicitly given

Object	*J*	*H*	*K*	*L*	*M*	*N*
R 4						
August 1983	12.26	11.89	11.03	9.85	–	–
R 50						
Glass (1977)	10.76(6)	10.46(6)	9.72(6)	8.09(6)	–	–
August 1983	10.72	10.41	9.58	8.00	6.82	–
Glass (1984)	–	–	–	–	–	5.17
R 66						
August 1982	10.22(20)	9.75(15)	8.90(10)	7.28(10)	6.25(25)	–
August 1983	10.02	9.68	8.83	7.32	6.45	
R 82						
AGL (1976)	11.51(7)	10.93(6)	9.76(5)	8.10(20)	–	–
August 1983	11.30	10.73	9.59	7.87	7.04	–
January 1984	11.39	10.84	9.69	7.51[a]	–	–
R 126						
AGL (1976)	10.01(5)	9.67(5)	8.67(5)	–	–	–
August 1983	9.99	9.64	8.64	6.88	5.58	–
January 1984	10.06	9.67	8.63	6.58[a]	6.35	–
Glass (1984)	–	–	–	–	–	4.26(7)
S 12						
August 1983	11.75	11.16	10.24	9.02:	–	–
January 1984	11.88	11.27	10.29	8.69[a]	–	–
S 22						
AGL (1976)	10.45(5)	9.92(5)	8.58(5)	–	–	–
BEN (1983)	10.74(25)	10.18(23)	9.01(19)	6.72(20)	6.79(60)	–
August 1983	10.34	9.77	8.46	6.47	5.72	–
Glass (1984)	–	–	–	–	–	4.43(5)
S 134						
August 1983	10.39	9.81	8.50	6.71	5.69	–

[a] Observed with the *L'*-filter ($\lambda_{eff} = 3.8\,\mu$m)

Table 4. Journal of IUE observations obtained in the low dispersion mode (for R 126 see Paper I)

Object	Image No.	Date	Camera	Exposure time [min]
R 4	12964	06.Apr.1982	LWR	60
	16699	06.Apr.1982	SWP	75
R 50	9659	08.Jan.1981	LWR	20
	10990	08.Jan.1981	SWP	30
R 66	12856	25.Mar.1982	LWR	8
	16619	25.Mar.1982	SWP	10
R 82	15115	28.Sep.1981	SWP	30
	11632	28.Sep.1981	LWR	20
Hen S 12	14450	11.Jul.1981	SWP	53
	11639	23.Mar.1982	LWR	40
Hen S 22	6867	08.Feb.1980	SWP	40
	6868	08.Feb.1980	LWR	22
	7821	08.Feb.1980	SWP	30.25
	13505	15.Mar.1981	SWP	12
	10147	15.Mar.1981	LWR	15
	14449	11.Jul.1981	SWP	30
Hen S 134	14447	11.Jul.1981	SWP	30
	11042	11.Jul.1981	LWR	20
	15117	28.Sep.1981	SWP	30
	11634	28.Sep.1981	LWR	20

2.2. Spectroscopic observations

All stars except R 4 have been observed between 1974 and 1984 with the coudé-spectrograph of the ESO 1.52-m telescope at La Silla/Chile with a linear dispersion of 20 Å mm^{-1}. These spectrograms are reproduced in Stahl et al. (1985) (henceforth referred to as the "Atlas").

In addition Hen S 22 has been observed in the red spectral range (5780 Å to Hα) on Sept. 29–31, 1979, using the ECHELEC spectrograph (cf. ESO User's Manual, 1979). Three spectrograms (linear dispersion 38 Å mm^{-1}) were recorded on a fine grain Ilford-G5-nuclear track emulsion using a Spectracon-tube with an S 20 photocathode. The projected slit width was 20 μm and the exposure times were 4^h36^m (P1589), 1^h37^m (P1591), and 30^m (P1595). All plates were digitized using a Grant-machine.

In July 20, and 25, 1983 R 50 and R 4 were observed with the CASPEC echelle spectrograph (d'Odorico et al., 1983) attached to the ESO 3.6-m telescope. The spectral resolution was $2\,10^4$. The exposure time was 1 hour both in the blue (3950–4950 Å) and the red (5820–6820 Å, R 50 only) spectral range. The spectrograph was equipped with a 31.6 lines/mm echelle grating, a 300 lines/mm cross dispersion grating and a F/1.5 camera. The reduction of the CCD frames was done with the image processing system of the Landessternwarte. Two additional CASPEC spectrograms of R 4 (covering the range 3920–4950 and 5730–6820 Å) were obtained on August 25, 1984. Furthermore, in Sept. 1, 1984 one CASPEC spectrum of R 66 in the red spectral range was secured. During this night we observed mainly blue spectra of other program stars. Therefore the 52 lines/mm echelle grating (which is recommended for observations at $\lambda < 4200$ Å) was used. This grating does not provide full spectral coverage beyond 5000 Å. We accepted the inter order gaps since it was our last night at the instrument and hence the chance to get a high quality red spectrogram (including H_α) of R 66. The reduction of this spectrum was carried out at ESO Garching, using the MIDAS echelle reduction package (Ponz, 1984).

In April 1984 red spectral range (5830 to 6730 Å) spectrograms of Hen S 134 and of R 82 were obtained at ESO, La Silla, using a Boller & Chivens spectrograph with a CCD detector attached to the Cassegrain-focus of the 2.2 m telescope. The linear dispersion of these spectrograms is 60 Å mm^{-1}, the spectral resolution about $3\,10^3$. The exposure times were 30^m for R 82 and 10^m and 3^m30^s for Hen S 134. The reduction was done at ESO/Garching using the IHAP-system.

Low resolution UV-spectrograms of all objects were obtained from the IUE data-bank of ESA in Villafranca, Madrid, Spain. The spectrograms cover the wavelength range from 1150 to 1950 Å (SWP) and 1950 to 3100 Å (LWR). Table 4 summarizes the relevant technical data of the IUE spectrograms.

3. Light variations

Luminous supergiants usually show irregular light variations which are particularly strong in the S Dor variables. Therefore, our photometric data base was carefully checked for light variations. Surprisingly no or only very small amplitude variations could be detected for the program stars. Even some of the "detected" variations (derived from a comparison of data obtained by different authors with different equipment) may be spurious and possibly may have been caused by different diaphragm sizes and other systematic effects as some of our programme stars are located in dense clusters in crowded parts of the MCs.

In detail our results on brightness variations are as follows: R 4 of the SMC, which has been observed photometrically since 1967, shows apparent variations in V of about 0.17 mag. However, this result is entirely based on a comparison of results obtained by different authors. Diaphragm effects could possibly produce systematic errors of the order of the apparent variations. The quoted value therefore should be regarded as an upper limit of the possible variability amplitude of this star only.

R 50 of the SMC has not shown any brightness variations exceeding 0.02 mag since 1960. Nor could any short term variations on a time scale of days be found in September 1983 (see Sect. 2) when R 50 was observed in the *uvby*-photometric system during 5 nights including three consecutive nights. The averaged results of these measurements are $y = 11^m.59 \pm 0.02$. $b - y = 0^m.20 \pm 0^m.03$, $c_1 = 0^m.51 \pm 0^m.05$, $m_1 = -0^m.01 \pm 0^m.05$. R 66 was observed differentially in the *uvby*-system. The observing sequence was *APB*, where A and B are comparison stars (A = HD 32762, $V = 8^m.2$, B = HD 31722, $V = 8^m.42$) and P is the programme star. The accuracy of the measurements was estimated from the variances of $B - A$ to $\sigma(y) = 0^m.011$, $\sigma(b - y) = 0^m.008$, $\sigma(C_1) = 0^m.015$ and $\sigma(m_1) = 0^m.009$. We determined for y, $b - y$, m_1, and c_1 the amplitudes A of variations by calculating the maximum of the absolute deviations of the single measurements from the mean value. We obtained $A(y) = 0^m.07$, $A(b - y) = 0^m.03$, $A(m_1) = 0^m.05$ and $A(c_1) = 0^m.08$. Amplitudes of comparable size have been found by Sterken (1977) for galactic late B-type supergiants.

In the case of R 82 brightness variations of the order $0^m.15$ in V within a decade are indicated. No significant colour variations were found. In Dec. 1981/Jan. 1982 this star was observed in *UBV* during 15 consecutive nights. Within this time interval variations of $\Delta V = 0^m.13$ and $\Delta(B - V) = 0^m.06$ were found. (In Table 1c the mean values of these measurements are given.) As pointed out in Paper I, in the case of R 126 no photometric variations could be detected. The upper limits were similar to R 50.

The few measurements of Hen S 12, which are available at present, do not allow a conclusion about variability, though a brightness variation in V of about $0^m.1$ might be implied by the data of Table 1d.

Hen S 22 has been checked for short term variability during two observing runs at ESO, La Silla in 1980 (11 consecutive nights) and 1981/82 (14 consecutive nights) with the same instrumentation (see Sect. 2). The results of each run agree excellently (Table 1e again gives the mean values). The variations during the single runs were not larger than $0^m.05$ in V. So neither significant short term variations nor variability on a time scale of one or two years were found. According to Table 1e variations on longer time scales up to $0^m.13$ may have occurred. However, these small apparent variations may again be explained by observational systematic errors.

In the case of Hen S 134 Table 1f seems to indicate rather large variations in V and $B - V$ of about $0^m.25$ and $0^m.20$, respectively. The B-magnitude however did not vary more than a few hundredths of a magnitude. Furthermore there is a systematic difference between the *UBV* and *UBVRI* measurements. An explanation for this could be found in the strong emission lines of Hβ and [O III] 4959, 5007 (see below). These lines are situated on the steep blue wing of the V-filter (cf. ESO User's Manual, Danks 1983). Since the V-filter used in *UBV* and *UBVRI* observations are not identical, small differences in the wavelength position of the blue wing could lead to the observed effect. We therefore conclude that the apparent effect in V is spurious and that the stable B magnitude shows that S 134 probably does not show significant light variations.

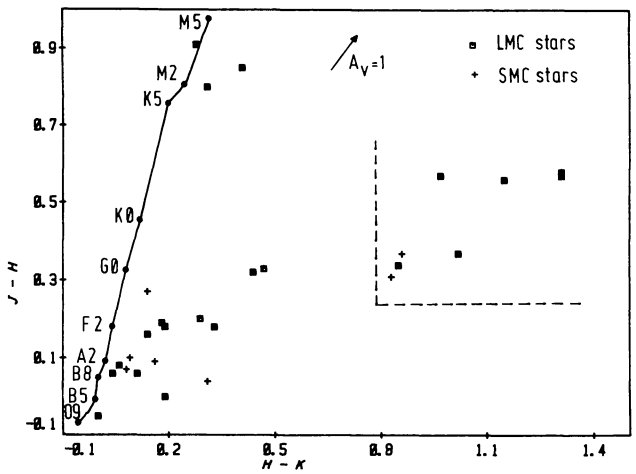

Fig. 1. $(J - H)$–$(H - K)$-diagram of emission-line stars in the MCs. The B[e]-supergiants are located to the right of and above the dashed line and obviously form a well separated homogeneous group

It thus follows that the B[e]-supergiants in the MC's have shown at most small photometric variations. The strongest variations were found for R 4 with $V = 0^m.17$. The observed brightness variations of the programme stars do not exceed those expected for typical early-type supergiants (Sterken, 1977). It should be stressed, however, that variations on very long time scales, i.e. a few decades and longer, cannot be excluded on the basis of our data.

The results of the IR-photometry, which are given in Table 3 also show no evidence for significant photometric variations.

4. Spectral energy distribution and basic stellar parameters

In Fig. 1 a $(J - H)$–$(H - K)$-diagram of the early-type emission-line stars of the Magellanic Clouds described in the "Atlas" are shown. The B[e]-supergiants form a clearly distinct group on the right-hand side of the $(J - H)$–$(H - K)$-diagram. Obviously their infrared excess in $(H - K)$ is so large that it cannot be explained by a late-type companion.

Figure 2 shows the continuous energy distribution of the B[e]-supergiants from the satellite (IUE) UV to the IR. The spectral energy distribution between the U- and V-band was derived from the magnitudes observed in August 1983. The conversion to absolute fluxes was done by applying the absolute calibrations of Bessell (1979) (*UBVRI*), and Wamsteker (1981) (*JHKLM*). Fluxes at 10 μm were obtained by converting the N-magnitude given by Glass (1984) with the absolute calibration of Thomas et al. (1973).

The infrared excess is clearly visible in all stars. We derived colour-temperatures for $H - K$, $K - L$, $L - M$ and, if available, $L - N$. The contribution of the stellar continuum in these wavelength bands was corrected by subtracting a Rayleigh-Jeans-distribution, which was normalized to the observed flux in J (1.25 μm). The temperatures calculated from the corrected colours are given in Table 5. The colour temperatures $T(H - K)$ and $T(K - L)$ lie between 1000 and 1200 K, while the $(L - M)$- and $(L - N)$-temperatures (for which approximately 700 K were

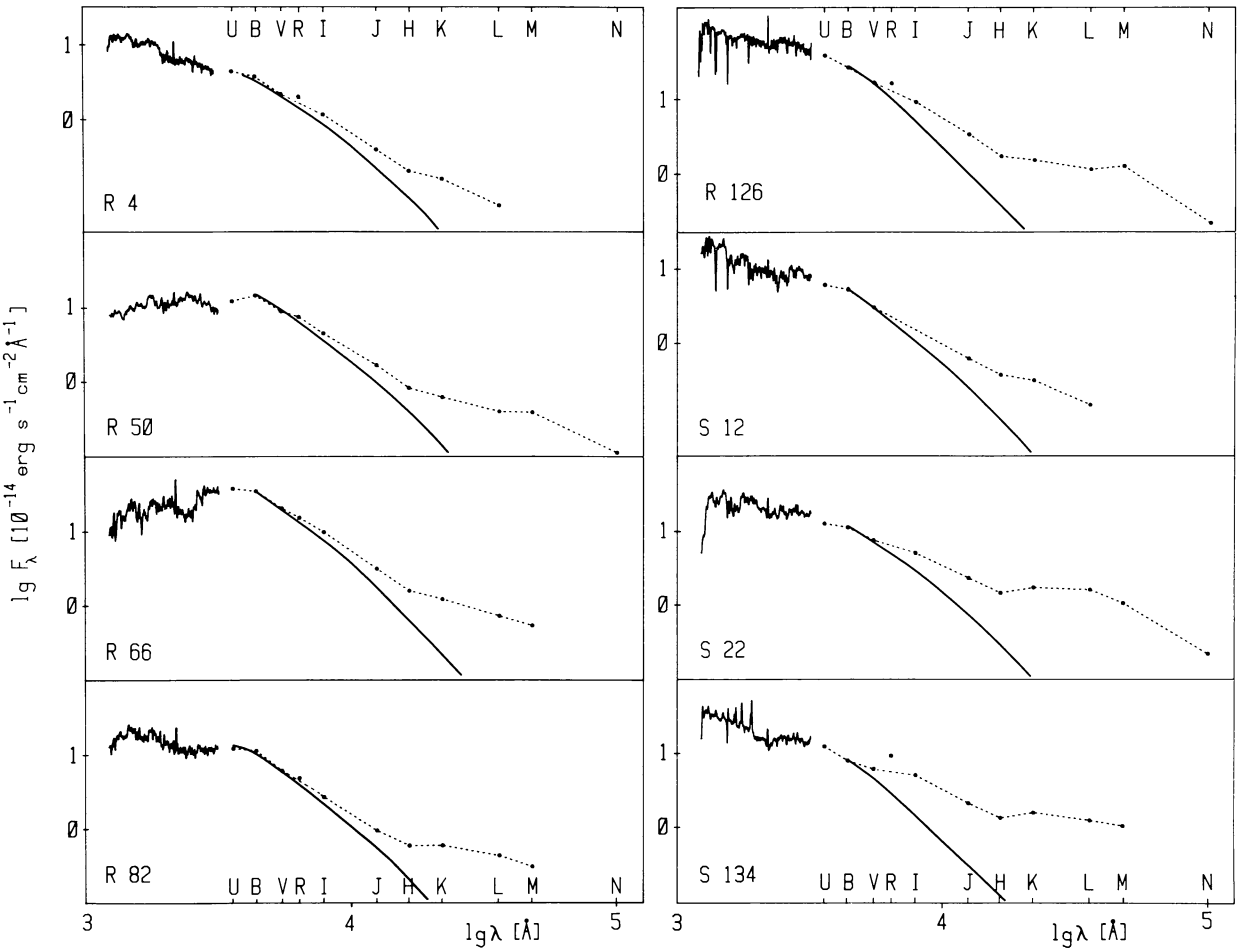

Fig. 2. Continuum energy distributions of the MC B[e]-supergiants from the satellite UV to the IR. The visual and IR-fluxes were deduced from broad-band photometry. An excess in $KLM(N)$ with colour temperatures of 900 K to 1200 K is clearly discernible. In order to better judge the amount of free-free envelope emission and circumstellar dust emission estimated visual and infrared fluxes for underlying Kurucz atmospheric models for the effective temperatures listed in Table 9 are also shown (full line). For this comparison the model atmosphere fluxes were dereddened with the E_{B-V} — values given in Table 9 and adjusted to the observed B and V values. The conspicuous excess in the R-band of most objects is due to the very strong Hα-emission

derived) are as a rule lower (apart for S 22). Such a wavelength dependence is e.g. expected in the optical thick case if the temperature in the circumstellar dust decreases with increasing radius.

In some cases the spectral types could be derived from photospheric absorption lines (see below). We furthermore used the continuum energy distribution between 1300 and 4400 Å (cf. Paper I) to derive the effective temperature and the reddening $E(B-V)$ by comparison with the dereddened continua of galactic supergiants. We applied the extinction law of Code et al. (1976) for the correction of the galactic foreground contribution (for which the generally accepted value of $E(B-V) = 0.05$ was assumed) and for the galactic supergiants. The reddening within the LMC and SMC was determined using the extinction laws of Nandy et al. (1981), and Rocca-Vollmerange et al. (1981), respectively.

Table 5. Colour temperatures in the infrared

Object	$T(H-K)$ [K]	$T(K-L)$ [K]	$T(L-M)$ [K]	$T(L-N)$ [K]
R 4	1150	1366	–	–
R 50	1130	1120	684	675
R 66	1230	1120	760	–
R 82	1084	1110	684	–
R 126	1045	1061	640	725
S 12	1193	1354	–	–
S 22	992	1009	969	875
S 134	996	1090	776	–

The UV-fluxes of the comparison stars were taken from two sources, namely Code and Meade (1979) (OAO) and Heck et al. (1984) (IUE). In Fig. 12 best fits of the comparison continua are shown for Hen S 22 and R 50. R 50 (and R 82 as well) shows a conspicuous flux deficiency longward of 2300 Å which will be discussed below. Table 9 summarizes the stellar $E(B-V)$ values and stellar parameters derived by these methods. The bolometric corrections were taken from Schmidt-Kaler (1982). The spectral type of Hen S 22, which was derived from the energy distribution, is consistent with the presence of the Si IV $\lambda\lambda$ 4089 4116-absorption lines, indicative of a hot stellar source.

The spectral energy distribution of the programme stars as shown in Fig. 2 are (in analogy to R 126, cf. Paper I) thought to consist of a B-type stellar continuum which dominates in the UV plus a (f – f)-(f – b)-contribution in the visual and near infrared

supposed to originate from the cool dense equatorial wind and an excess at about 3 μm which is due to the radiation of circumstellar dust with a typical temperature of 900–1000 K. Likewise the dust is supposed to form in the outer parts of the cool equatorial wind.

The equatorial (f – f)–(f – b)-radiation can also account for the fact that absorption features are generally weak or even absent. This radiation causes a veiling which according to model calculations (for disk configurations of normal B[e]-stars) of Poeckert and Marlborough (1978) increases with decreasing inclination angle.

Whether the $E(B-V)$ values derived above are due to interstellar absorption only or whether a circumstellar contribution may be important, cannot be decided from the continuum energy distribution alone. However, four stars of our sample are obviously members of associations (Lucke and Hodge, 1970), namely R 82 of LH 35, R 126 of LH 93, Hen S 22 of LH 38, and Hen 134 of LH 104. Lucke (1974) derived the mean reddening of LH 93, LH 38, and LH 104 to $E(B-V) = 0.18$, 0.09, and 0.23, respectively. The agreement of our derived $E(B-V)$-values with those derived for the associations is reasonable for R 126 and Hen S 134. On the other hand, a large discrepancy is found in the case of Hen S 22, which we ascribe to additional circumstellar absorption. Since our programme stars are supposed to form a rather homogeneous group this different behaviour at a first glance appears to be surprising. An explanation will be given below.

The determination of $E(B-V)$ has been made with the assumption that the normal interstellar extinction laws apply. Since circumstellar absorption for which the extinction law is unknown is likely to play a role at least in some cases, some uncertainty is introduced into the derived values of the stellar parameters. However, in four cases the spectral type was also determined from photospheric lines. As shown in Table 9 the agreement with the spectral type derived from the continuum distribution is good. This makes us confident in our determination of the stellar parameters.

5. Remarks on and interpretation of the individual stellar spectra

The spectrum of R 126 has been described already extensively in Paper I, which also contains a tentative interpretation of the observed spectral properties. Therefore, in this chapter we shall compare the spectra of the other B[e]-stars with that of R 126 and with the scenario outlined in Paper I. In doing so, we shall start with those spectrograms which resemble R 126 most closely. In detail we wish to make the following remarks on the individual programme stars:

Table 6. Doppler velocities of the emission lines of Hen S 134 as determined from the half line widths at half maximum ($v_{1/2\,\mathrm{FWHM}}$)

Line	v ($\frac{1}{2}$ FWHM) [km s^{-1}]
He II	400
H	50
He I	48
Si II	42
[O III]	38
[Ne III]	36
Fe II	36
[Fe II]	27

5.1. *Hen S 134*

The blue spectrum (as shown in the "Atlas") is characterized by a large number of emission lines. Absorption lines are not visible on our coudé-spectrogram. A strong Balmer continuum excess is present. The strongest lines are due to the Balmer series, visible up to H22. Furthermore, emission lines of He I, Fe II, Si II and Ca II are present. The nebular lines [Ne III] 3869, 3969 Å and [O III] 4959, 5007 and 4363 Å are very prominent. [O II] 3726/29 are faint. In addition we could identify weak [Fe II]-lines. [Fe II] 4244 is approximately half as strong as Fe II 4233. The presence of He II 4686 in emission is an indication of a hot underlying star. This line is very broad (full width at continuum level ≈ 1000 km s^{-1}). The emission lines of various ions show different line widths. The half half-widths are listed in Table 6. They lie between 50 km s^{-1} for H and He I and 35 km s^{-1} for Fe II. The Si II-lines are slightly broader than the Fe II-lines, while the forbidden lines of Fe II are the sharpest lines with 27 km s^{-1}. The errors of these values are about $\pm 10\%$. He II 4686 is, as mentioned above, exceptionally broad.

Likewise in the red spectral range shown in Fig. 3 no stellar absorption lines were found. Beside Hα we identified strong lines

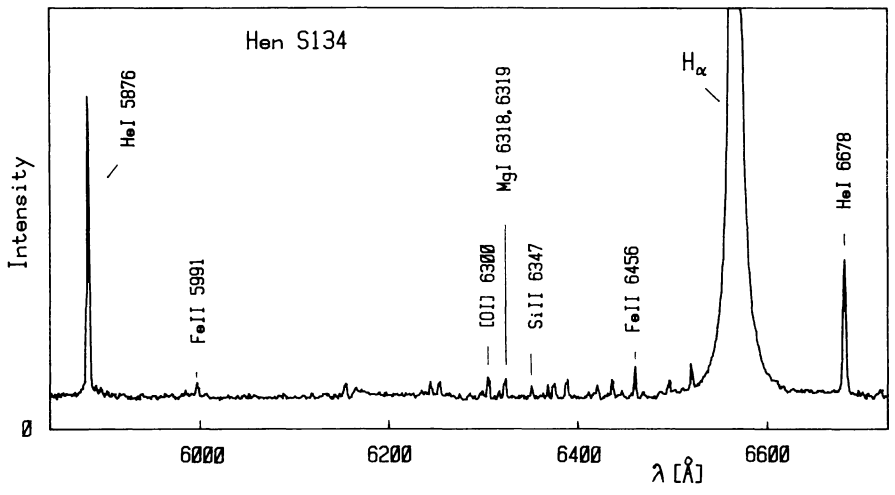

Fig. 3. Section of the red spectral range of Hen S 134

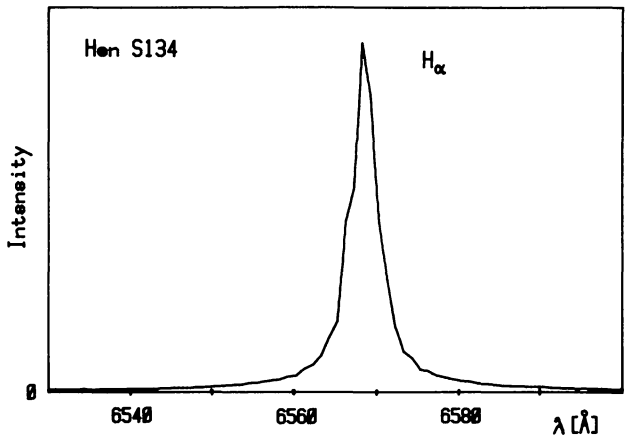

Fig. 4. Hα-profile of Hen S 134. An unresolved absorption feature may be indicated by the hump in the blue wing of the emission feature

of He I as well as numerous weak lines of Fe II. Furthermore [O I] 6300, Mg I 6318 and Si II lines are present. [N II] 6584, 6548 lines could not be detected. The Hα-profile is shown in Fig. 4. It is clearly asymmetric, exhibiting a hump on the blue wing which could be indicative of an unresolved absorption component. The hump is blueshifted relative to the maximum of the emission by about 90 km s^{-1}.

We measured heliocentric radial velocities on the coudé-spectrogram and obtained for the Balmer lines $+261 \pm 9$ km s^{-1}, for He I $+264 \pm 8$ km s^{-1}, for Fe II and [Fe II] $+267 \pm 10$ km s^{-1} and for [Ne III] and [O III] $+258 \pm 9$ km s^{-1}. The mean value is $+264 \pm 4$ km s^{-1}. This agrees well with the measurements of Ardeberg et al. (1972).

The line spectrum in the UV was discussed by Shore and Sanduleak (1983). One of the most important facts is the presence of P Cygni profiles of N V, C IV and Si IV. The widths of the absorption components indicate outflow velocities of the order of 2300 km s^{-1}. This sharply contrasts with the appearance of the visual spectrum where only narrow emission lines are present. Hence Hen S 134 shows, like R 126, a "hybrid spectrum" with sharp emission lines (30–50 km s^{-1}) of singly or doubly ionized elements in the visual wavelength region and broad blueshifted absorption components of highly ionized species, which imply high expansion velocities (2300 km s^{-1}). The dependence of the emission-line width on the excitation potential which was found for R 126 exists also for Hen S 134. Shore and Sanduleak (1983) proposed a spherically symmetric model for Hen S 134. Following the discussion in Paper I for R 126, we suggest that our two-component-model also provides a likely explanation of the hybrid spectrum of Hen S 134. The very broad He II 4686 line is supposed to originate in the hot high velocity component of the wind. Like in the case of R 126 we presumably observe the disk of Hen S 134 under a small inclination angle (i.e. "pole-on").

5.2. *Hen S 22*

The blue spectrum, which has been described in detail by Muratorio (1978), is dominated by the strong emission lines of the Balmer series and a great number of permitted and forbidden lines of singly ionized iron. Balmer continuum emission is also present. The Balmer lines from Hα (see Fig. 5) to Hδ show P Cygni profiles of Beals's type III, while the higher Balmer lines exhibit pure emission lines without absorption components. The Balmer line profiles appear to be variable if compared with the profiles published by Muratorio (1978). His spectrograms show P Cygni profiles from H8 to H31 with an absorption component which is blueshifted by -70 km s^{-1} relative to the [Fe II]-lines. We note that this cannot be a resolution effect since our blue spectrograms were taken with the same instrument. The relative strength of forbidden and permitted Fe II-lines however has not varied. In accordance with Muratorio (1978) we found an intensity ratio $I(4244)/I(4233)$-1. The line widths of the Fe II- and [Fe II]-lines were determined to 55 km s^{-1} (FWHM). Further forbidden lines in the blue spectral range are [S II] 4069 and possibly [Fe III] 4658. The typical nebular lines are not present, however.

The systemic velocity was determined from the Fe II- and [Fe II]-lines to $+293 \pm 3$ km s^{-1} in good agreement with Muratorio's (1978) value of $+290$ km s^{-1}. Radial velocities of the Balmer line components are summarized in Table 7.

An important new finding is the detection of two faint, presumably photospheric, absorption lines near Hδ being due to Si IV 4089, 4116 (Fig. 6). The radial velocities $+318$ km s^{-1} (λ 4089 Å) and $+297$ km s^{-1} (λ 4116 Å), are in good agreement

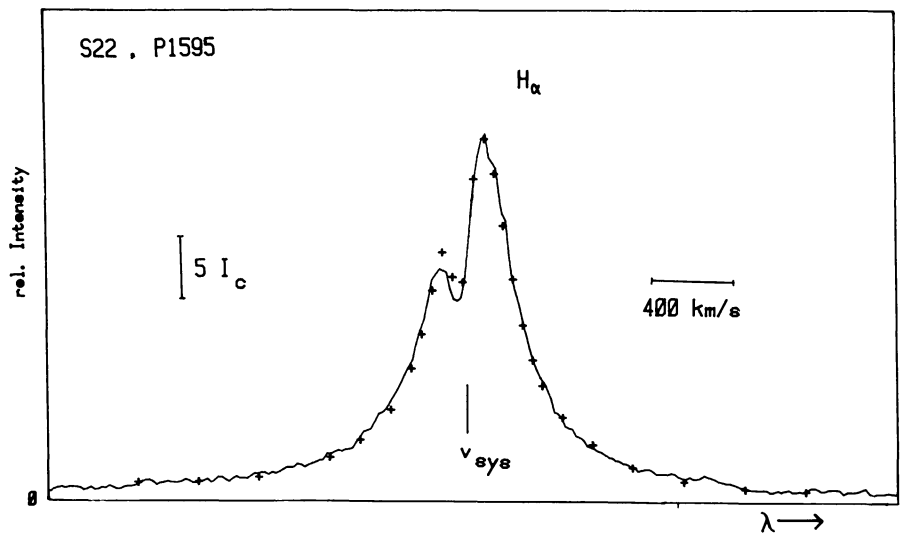

Fig. 5. Hα-profile of Hen S 22. The absorption component is blue shifted by -87 km s^{-1} with respect to the systemic velocity. The broad wings are explained by incoherent scattering of the line photons by free electrons. A theoretical profile calculated with this assumption is indicated by the crosses (cf. Sect. 4)

Table 7. Heliocentric radial velocities of the Balmer line components of Hen S 22

Line	v (em, blue) [km s^{-1}]	v (abs) [km s^{-1}]	v (em, red) [km s^{-1}]
Hβ	199	252	347
Hγ	204	261	333
Hδ	224	243	327
Hε	–	–	324
H8	–	–	326
H9	–	–	316
H10	–	–	329
H11	–	–	323
H12	–	–	329

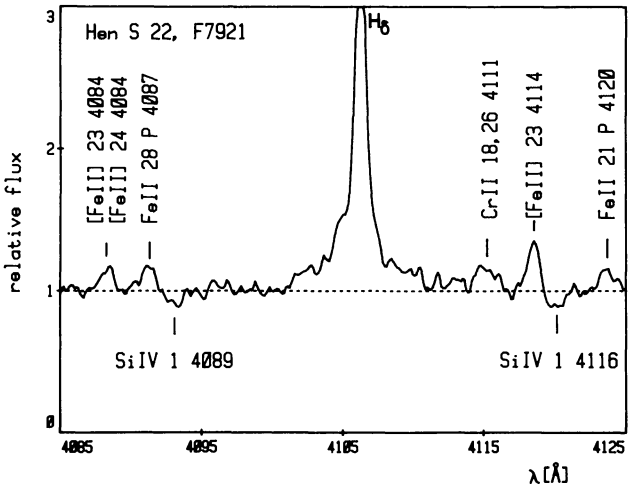

Fig. 6. Section of the blue spectrum of Hen S 22 around Hδ. Two faint presumably photospheric absorption lines of Si IV (1) indicating a hot underlying star are discernible. The continuum level is indicated by the dashed line

with the systemic velocity. The slight differences are probably due to the fact that both lines are contaminated by nearby emission lines (see Fig. 6). Note that no trace of the Si IV lines is discernible in the spectra published by Muratorio (1978). This may confirm that spectral variations have occurred in S 22 within the past few years.

In the red wavelength range (two sections of which are shown in Fig. 7) beside Hα, emission lines of Fe II, mainly of multiplets 40, 46 and 74, were found. Furthermore emission lines of He I, Si II, Mg II and Fe II could be identified. [O I] 6300 is the second strongest line in the red wavelength range. [N II]-lines are not present.

The radial velocities of the emission lines in the red wavelength region (for which a mean value of $+291 \pm 3$ km s^{-1} was determined) agree well with the velocities derived from the lines in the blue range.

The expansion velocity derived from the violet-shift of the absorption component of Hα is -87 km s^{-1} (with $v_{sys} = +293$ km s^{-1}). This agrees well with Muratorio's (1978) value of -70 km s^{-1} which he derived from the higher Balmer lines. However, on a spectrogram obtained three years later we measured an expansion velocity of only -40 km s^{-1} from Hβ, Hγ, Hδ which could e.g. be due to a variable expansion velocity, to the ejection of discrete shells, or to variations of the optical depth of the line forming region on time scales of years. Hα and Hβ of S 22 show very extended wings. In the case of Hα (see Fig. 5) the total width is about 2000 km s^{-1}. However it is not necessary to assume the presence of macroscopic velocities of this amount to explain the wings as suggested by Bensammar et al. (1983). Rather these wings can be ascribed to incoherent Thomson scattering of line photons by free electrons. We applied the method

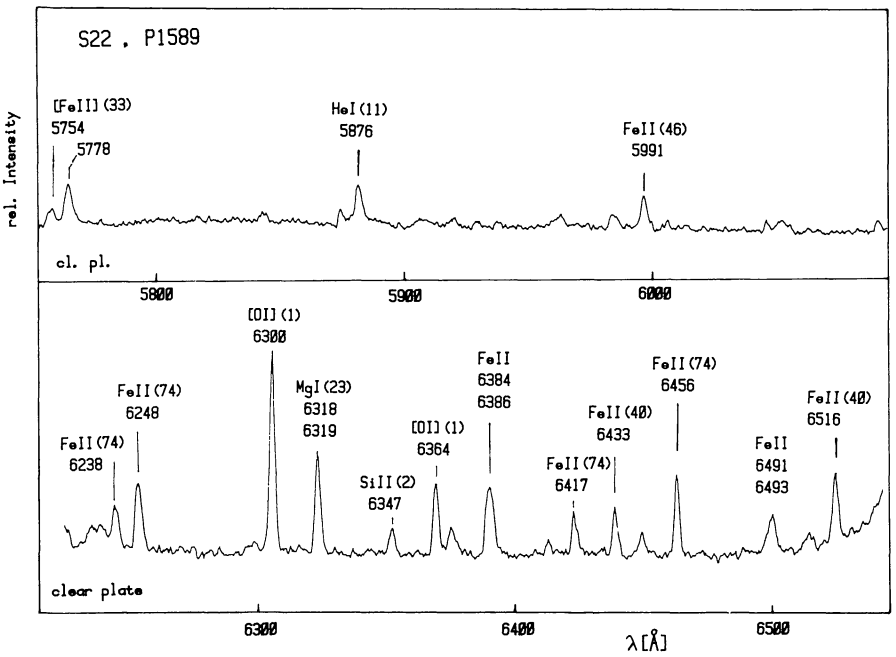

Fig. 7. Sections of the red spectrum of Hen S 22

described by Wolf et al. (1981) to interpret the wings of Hα. The result of the computations is shown in Fig. 5 (crosses). The theoretical profile has been fitted to the observed one yielding an electron scattering optical depth of $\tau_e = 1.25$ and an electron temperature of $T_e = 5240$ K. This temperature agrees well with the excitation temperature of the metastable Fe II-levels, for which Friedjung and Muratorio (1980) found $T_{ex} = 5060$ K.

An estimate for the radius of the dust region can be obtained as described in Paper I. The excess flux in the infrared was obtained by subtracting a (f-f)-envelope emission and a photospheric contribution approximated by the Rayleigh-Jeans law, normalized to the flux at J (1.25 μ). For the J-band the dust radiation is expected to be negligible. With $T_{dust} \approx 1000$ K we derived from the excess in K a maximum and a minimum radius of $265\,R_*$ and $169\,R_*$, respectively. The maximum radius was obtained by postulating black particles and the dust region being in radiative equilibrium with the radiation from the star; the minimum radius was estimated assuming that the IR-radiation is emitted by an optically thick, spherically symmetric envelope (cf. also Eqs. (1) and (2) of Paper I). It is interesting to compare these results to the radii of the Fe II- and [Fe II]-line emitting region which were derived by Friedjung and Muratorio (1980). However, since Friedjung and Muratorio used $E(B-V) = 0.09$ their derived fluxes are lower by about a factor of 2 than those calculated with our $E(B-V)$ of 0.30. Applying this factor we derive an upper limit for the Fe II-line emitting region of $146\,R_*$. For [Fe II] Friedjung and Muratorio (1980) obtained a radius larger by a factor 1.7 than for Fe II, i.e. $248\,R_*$. Hence the approximate radii of the dust forming region and of the Fe II- and [Fe II]-line emitting region are of the same size.

Bensammar et al. (1983) identified violet displaced absorption features of Si IV and C IV in the IUE spectrum of S 22. Precise radial velocities cannot be derived from low dispersion IUE spectra. But since the centres of these absorption features are blueshifted by about -1300 km s^{-1} whereas some (presumably interstellar) features like C II 1335, Si II 1526, Fe II 1608 and Al II 1670 show velocities between -150 and $+350$ km s^{-1} we regard a considerable expansion velocity of the order of 1000 km s^{-1} as real. Violet displaced absorption features of highly ionized species in the IUE spectrum and narrow emission lines of singly ionized ions in the visual wavelength range make Hen S 22 another example of the hybrid-spectrum B[e]-supergiants.

Bensammar et al. (1983) suggested for this particular star an accretion disk model of a young star with a very short evolutionary time. Hen S 22 would thus be a unique case in the LMC. Since more objects with the described spectral characteristics are known to be members of the LMC our two-component wind model appears to be a more likely explanation for S 22. The presence of Fe II absorption features in the UV as identified by Bensammar et al. (1983) could be interpreted by absorption in the equatorial wind, assuming a larger inclination angle than in the cases of R 126 or Hen S 134. In this case circumstellar dust may also occur along the line-of-sight, which would explain the relatively high reddening if compared with the mean reddening of the association of which S 22 is a member.

5.3. *R 50*

In contrast to Hen S 134 and S 22 the SMC star R 50 shows strong absorption lines in the optical spectrum and strong Balmer continuum absorption. A list with line identifications has been given by Muratorio (1981). Whereas He I 4472 is already recognized as an absorption line on each individual coudé-spectrogram, some fainter, yet very important, absorption lines became only discernible after the superposition of four coudé-spectrograms. These lines are He I 3819, 4009, 4026, 4388 and 4713 (which were already identified by Muratorio, 1981) and particularly N II 3995 and Si II 4128, 4131. A spectral type of (B2–3) can be deduced from the line intensity ratios.

The systemic velocity was derived from the Fe II-lines to $+191 \pm 4$ km s^{-1} in good agreement with velocities derived by Muratorio (1981) ($+187$ and $+195$ km s^{-1}), Feast et al. (1960) ($+184$ km s^{-1}), Maurice (1976) ($+193 \pm 6$ km s^{-1}). For the Balmer line emission components of Hβ to H8 we derive radial velocities of $+243 \pm 6$ km s^{-1} whereas the absorption components of H11 to H27 yield 180 ± 3 km s^{-1}. No Balmer progression was detected on our plates. The maximum expansion velocity measured at the blue edges of the Balmer absorption lines from Hγ to H15 was measured to -95 ± 10 km s^{-1}.

The high resolution and high S/N-ratio CASPEC-spectrograms revealed several unexpected spectral properties: In Fig. 8 three sections of the blue spectrogram are shown. Apart from the lines already known from the coudé-spectra we found a large number of Ti II and Cr II absorption lines which are much sharper than the photospheric lines mentioned above. Only the strongest of these lines (e.g. Ti II (13)3757–61, Cr II 4559) are already discernible on our coudé spectrograms. Furthermore, the permitted emission lines of Fe II show a central absorption component. Yet the [Fe II]-lines have no double peak structure. We determined the systemic velocity from the [Fe II]-lines and obtained $+184 \pm 4$ km s^{-1}. For the sharp Ti II- and Cr II absorption lines we measured radial velocities of 179 ± 4 km s^{-1}. The central absorptions of Fe II show a velocity of $+177 \pm 4$ km s^{-1}. In the red spectral range Hα, emission lines of Fe II (mainly of multiplets 40, 46 and 74), [O I] 6300, 6364 and Mg I 6318–19 are present. The Fe II lines again exhibit a central absorption. Furthermore, the Na I D lines show a complex P Cygni-type structure (see Fig. 9) with an emission component at a radial velocity of $+212$ km s^{-1}, galactic and SMC interstellar components and a probably circumstellar absorption component at a radial velocity of $+151$ km s^{-1}. He I 5876 is present as absorption line with a radial velocity of $+146$ km s^{-1}.

We measured the widths (FWHM) of Fe II, [Fe II] and [O I] emission lines to 70 km s^{-1}, 40 km s^{-1} and 44 km s^{-1}, respectively. From the blue edge of the absorption component of Hδ we derived an expansion velocity of -87 ± 15 km s^{-1} which agrees well with the value derived from the coudé-spectrograms.

The broad wings of Hα, Hβ, Hγ are again interpreted by incoherent electron scattering. With the method cited above we derived an optical thickness $\tau_e = 0.8$ and an electron temperature $T_e = 4200$ K from $H\beta$ and Hγ (using the coudé-spectrograms). Further information about the physical structure of the stellar environment was derived from a curve-of-growth analysis of the Ti II shell lines. The gf-values were taken from Kurucz and Peytreman (1975). The comparison with the theoretical curve-of-growth of Unsöld (1955) yielded an excitation temperature of $T_{ex} = 10\,000 \pm 1000$ K and a microturbulence parameter of 1.7 ± 0.3 km s^{-1} (see Fig. 13). Note that the thermal velocity of Ti II-ions is 1.86 km s^{-1} at $T = 10^4$ K.

The [Fe II] line intensities were used to obtain another estimate of the reddening and to deduce the excitation temperature

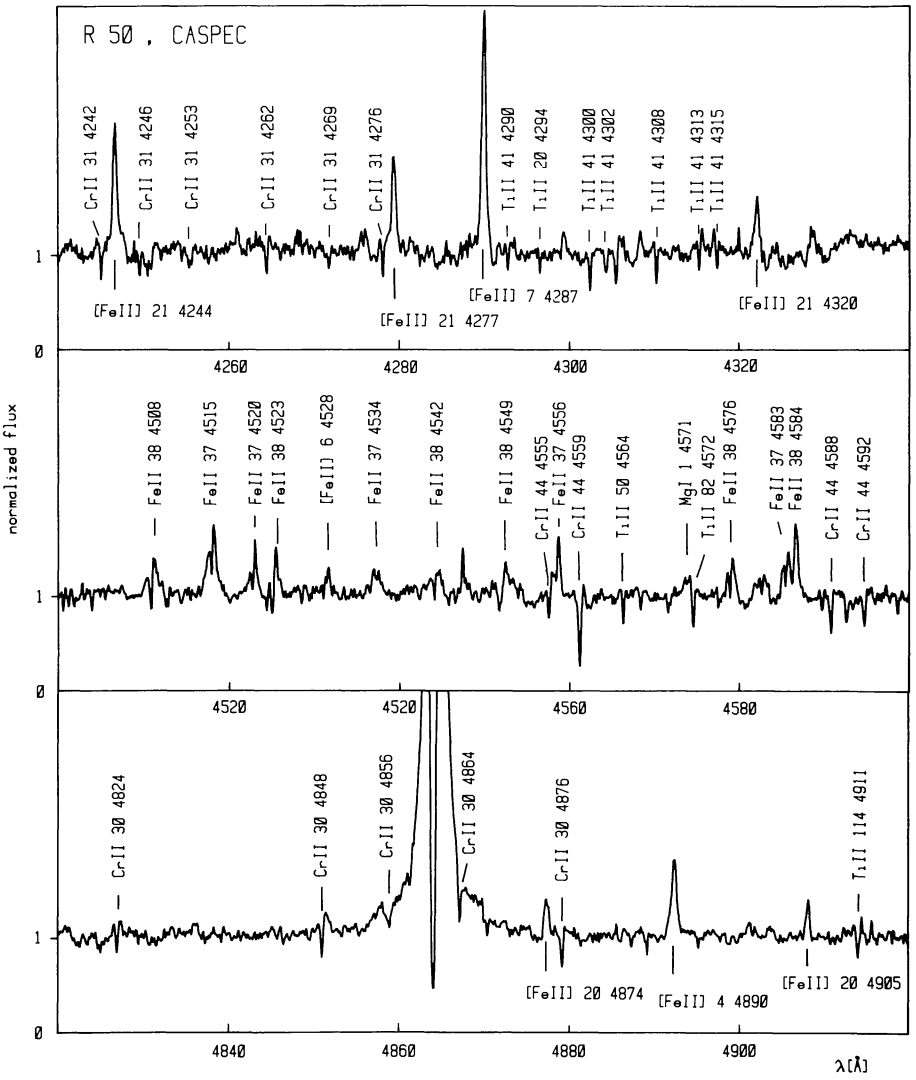

Fig. 8. Three sections of the CASPEC-spectrogram of the blue spectral range of R 50. Note the numerous very sharp "shell"-type absorption lines of Ti II and Cr II which are blue shifted by only $-5\,\mathrm{km\,s^{-1}}$ relative to the [Fe II]-lines. The permitted Fe II-emission lines show a central absorption feature with the same shift

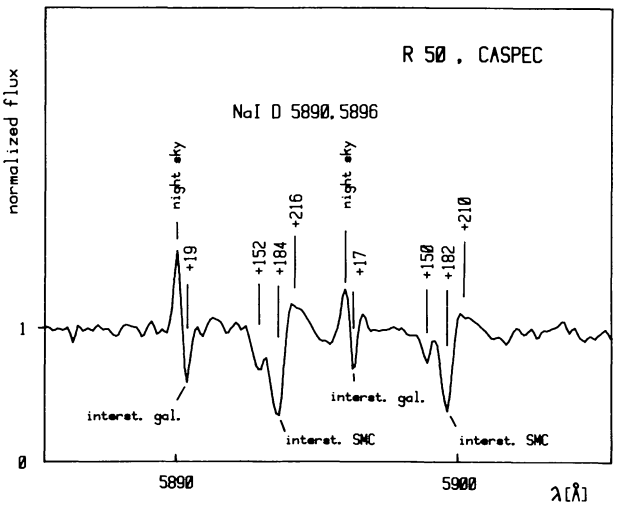

Fig. 9. Section of the red CASPEC-spectrogram of R 50 showing P Cygni profiles of the NaI D doublet. The absorption components are split into two subcomponents, originating in the SMC interstellar matter and in the circumstellar gas, respectively

from the metastable upper levels by applying the relation

$$\log(I_{ij}\lambda_{ij}/g_iA_{ij}) = \log(N_i/g_i) + \text{const} \quad (1)$$

(e.g. Caputo, 1971) where N_i is the population number of the upper level, A_{ij} and λ_{ij} are the transition probability and wavelength, g_i is the statistical weight of the upper level, $I_{ij} = W_{ij}F_c$ is the intensity of the line with the equivalent width W_{ij} and the dereddened continuum flux F_c at the line frequency. An estimate for the reddening can be obtained from the line intensities of multiplets 6 and 20 of [Fe II] at 4400 and 4900 Å, respectively, which originate from the same upper level. Hence the left-hand sides of Eq. (1) should yield the same value for both multiplets. With the A-values of Garstang (1962) we derived from the CASPEC-spectrogram $E(B-V) = 0.15$. For this procedure the $UBVRI$-photometry was used to calibrate the CASPEC data. Our value is in good agreement with the $E(B-V)$ obtained from the flux distribution in the UV. In Fig. 14 the normalized line intensities given by the left-hand side of Eq. (1) are plotted against the excitation potential of the upper level. From a least-square-fit we finally derived an excitation temperature of $T_{ex} = 6450\,\mathrm{K}$. It thus appears that a radial temperature stratification exists in the

circumstellar environment of R 50. The forbidden [Fe II] lines and the broad wings of the Balmer lines due to electron scattering would originate in the cooler rarefied outer regions whereas the absorption lines of Ti II and probably also the central absorption components of Fe II would be produced in the inner denser and hotter regions. However, we should like to note that NLTE effects may play an important role in the extended regions around R 50 which make temperature derivations from population numbers unreliable.

The line spectrum of R 50 as observed with CASPEC has many features in common with the peculiar, non-supergiant shell stars like HD 45677 (cf. Swings, 1973), in particular the Fe II emission lines with a central absorption core. The Balmer lines exhibit the typical P Cygni profiles of Beals' type III with a shell absorption reaching below the continuum level. The superimposed absorption-line spectrum with sharp lines of Ti II and Cr II resembles typical spectra of the "classical" (less luminous) shell stars such as 48 Lib.

Within our two-component stellar wind model R 50 can thus be regarded as a case of an "edge-on" object. The flux deficiency longward of 2300 Å up to the Balmer limit (see Fig. 12) can be understood as Balmer continuum absorption in the cool and dense equatorial wind. A Balmer jump which is too large for the spectral type considered is also known from classical Be-stars, e.g. from ζ Tau (Schild, 1976). With the $E(B-V)$ given above we derived in the case of R 50 $(U-B)_0 = -0.50$ corresponding to a spectral type B9 of the *circumstellar disk* configuration, in accordance with the excitation temperature of the metallic absorption line spectrum (Ti II: $T_{ex} = 10{,}000$ K). Likewise we regard the spectral type B9: Iaep derived by Ardeberg and Maurice (1977) as being due to this equatorial disk whereas the underlying photospheric absorption line spectrum (see above) is characteristic for an *early* B star.

5.4. R 82

The close resemblance of the line spectra of R 82 and R 50 has been stressed by Maurice (1976) and by Muratorio (1981) who gave an extensive list of line identifications. The intensity tracing of our coudé-spectrogram is shown in the "Atlas". The spectrum of the red region is reproduced in Fig. 10. The lines of the Balmer series show P Cygni profiles from Hα to H9 (Beal's type III from Hα to Hδ), while the higher Balmer lines are present only in absorption. The Fe II- and in particular the [Fe II]-lines are somewhat weaker than in R 50. The ratio $I(4244)/I(4233)$ is about 1. Some of the stronger Fe II emission lines appear to be split into two emission components as was found for R 50. Muratorio (1981) also reports on such line profiles. Further forbidden lines found in the spectrum are [S II] 4069 and a weak [O II] 3726–29.

As in the spectrum of R 50 we could identify absorption lines of He I, N II and Si II. In contrast to R 50 Mg II 4481 could also be detected. This might be due to the generally greater strength of the absorption lines in R 82. They appear to be broader than the absorption components of the Balmer lines. The spectral type which we deduced from the relative intensities is B2. Furthermore sharp absorption lines of Ti II 3759, Ni II 3769, Cr II 3678 (blend) are present.

The red spectral range (Fig. 10) is dominated by a strong Hα-emission line. Most other emission lines are due to Fe II. In addition, Mg I 6318–19, Si II, and [O I] λλ 6300, 6364 are present. [O I] λ 6300 is the second strongest line in the red range. The intensity of this line is possibly variable, since Shore and Sanduleak (1984) report only of weak [O I]-emission. Allen and Glass, however, found, in accordance with our spectrum, a strong O I-line. These "variations" however can also be due to different settings of the spectrograph slit on an extended nebula. He I 5876, 6678 are present as absorption lines.

The measured heliocentric radial velocities are summarized in Table 8.

Table 8. Heliocentric radial velocities of R 82 measured in the coudé-spectrogram

Line	v_{em} [km s^{-1}]	v_{abs} [km s^{-1}]
Hβ-Hε	316	–
Hβ-H27	–	236
[Fe II]	252	–
Fe II	205/288	–
Ca II K	326	234
[O II]	267	–
He I	–	257
Si II	–	243
Mg II	–	230

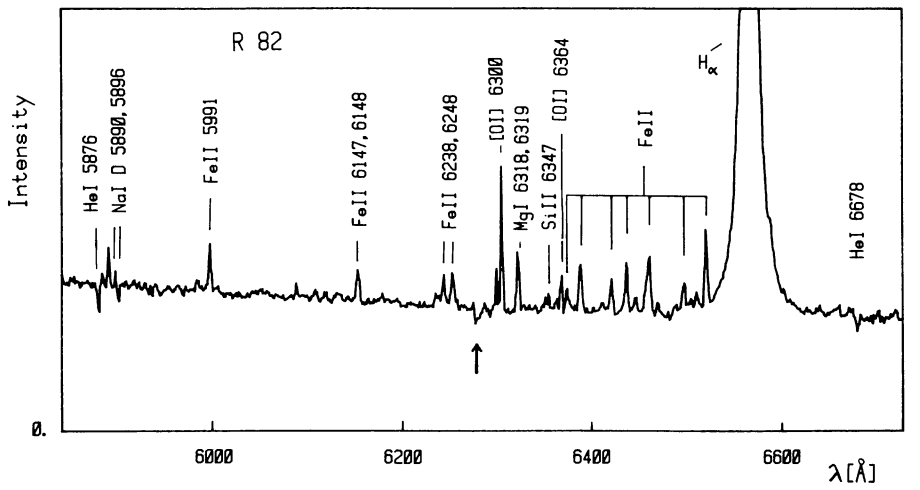

Fig. 10. Section of the red spectral range of R 82. Apart from numerous emission lines, mainly of Fe II, absorption lines of He I are visible. The absorption feature marked by an arrow is due to the atmospheric O_2-band at λ 6277

The close similarity of the line spectra of R 50 and R 82 implies that the latter star may also be regarded as a case of a two-component wind object seen "edge-on". The presence of narrow absorption lines of Ti II, Cr II and Ni II indicates a shell-type absorption line spectrum as in R 50. Furthermore the Balmer jump is also slightly stronger in absorption compared to the continuum energy distribution of the B2-type star which is indicated by the photospheric absorption spectrum.

5.5. *R 66*

The blue spectrum of R 66 was extensively discussed by Stahl et al. (1983). In contrast to all other members of our sample this star does not show forbidden lines in the blue spectral range. But its classification as a B[e]-star is justified by our finding of the very strong (70% of the adjacent continuum) [O I] λ 6300-line. (Due to the inter order gap between 6360 and 6380 Å [O I] λ 6364 could not be observed.) In addition a faint (7% of the adjacent continuum) [S II] 6716 line was identified.

The width (FWHM) of [O I] 6300 for which 30 km s^{-1} were measured is considerably smaller than the one measured for the Fe II-emission lines (50 km s^{-1}) of the CASPEC spectrum. Stahl et al. (1983) suggested a decelerated wind velocity law for an interpretation of the spectroscopic properties of R 66. R 66 exhibits a hybrid spectrum however as well: Unshifted sharp emission lines of Fe II and still sharper forbidden lines of [O I] and [S II] are contrasted by high velocity absorption components with a maximum expansion velocity of $v_{max} \approx 300$ km s^{-1}. This velocity is typical for the stellar winds of a B8 supergiant, which is the spectral type derived for R 66 by Stahl et al. Hence R 66 may belong to the same category as R 126 (Paper I), the main difference being the later spectral type of R 66. We prefer this hypothesis since it would allow a uniform description of all MC B[e]-supergiants, although we note that the decelerated wind model cannot be excluded. Unlike the prototype R 126, where a pure emission line spectrum is observed in the visual, R 66 shows pronounced P Cyg profiles. This can be explained by assuming that the disk-like object is seen under a larger inclination angle.

5.6. *Hen S 12*

The complete coudé-spectrogram of the blue wavelength range is again shown in the "Atlas". In Fig. 11 the Balmer-lines from Hα to H8 are reproduced. P Cygni-profiles are present from Hβ to H8. H9 is purely in absorption. (The higher members of the Balmer series are underexposed.) The large strength of H8 is presumably due to a blend with He I 3888. This line arises from the metastable 2^3S-level and tends to be enhanced in objects with extended atmospheres (cf. Struve and Wurm, 1938). The absorption components of the Balmer lines appear to be separated from the emission component (see Fig. 11). Similar profiles have been found for the Fe II-lines in R 66 (cf. Stahl et al., 1983).

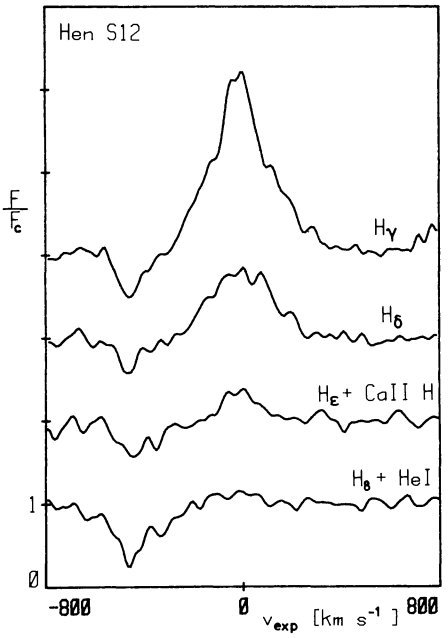

Fig. 11. Profiles of the Balmer lines of Hen S 12

In addition to the Balmer-lines, emission lines of Fe II and [Fe II] could be identified. The forbidden lines are considerably weaker than the permitted ones. [Fe II] 4287, 4359, 4413–16 are clearly present, however. Photospheric absorption lines cannot be detected at our relatively low S/N-ratio. The systemic velocity (derived from the Fe II- and [Fe II]-lines to $+285 \pm 10$ km s^{-1}) is in good agreement with Ardeberg et al. (1972), who give $+284$ km s^{-1}. For the emission components of the Balmer lines we obtained $+290 \pm 9$ km s^{-1}. The absorption components have a velocity of -167 ± 6 km s^{-1}. This yields an expansion velocity in the line centres of -450 km s^{-1}. The maximum expansion velocity, which was measured from the blue edges of the Balmer line absorption components, is -550 km s^{-1}. For a description

Table 9. Stellar Parameters of the B[e]-Stars

Object	*SP*[a]	*SP*[b]	$E(B-V)$	T [10^3 K]	M_{bol} [mag]	R [$R_\odot$]	M [$M_\odot$]
R 4	B0–0.5	B0.5	0.20	23–26	$-8.8 \ldots -9.3$	32	30–40
R 50	B2–3	B3	0.15–0.20	17	-9.5	81	40–50
R 82	B2	B3	0.20	18.5	-8.8	50	30
Hen S 12	–	B0.5	0.20–0.25	23	-8.6	30	25–30
Hen S 22	–	B0–B0.5	0.25–0.30	23–26	$-9.7 \ldots -10.2$	49	50–55
Hen S 134	–	B0	0.20–0.25	26	-10	45	60
R 126	–	B0.5	0.25	22.5	-10.5	72	70–80
R 66	B8	B8	0.12	12	-8.9	125	30

[a] Spectroscopic
[b] Continuum

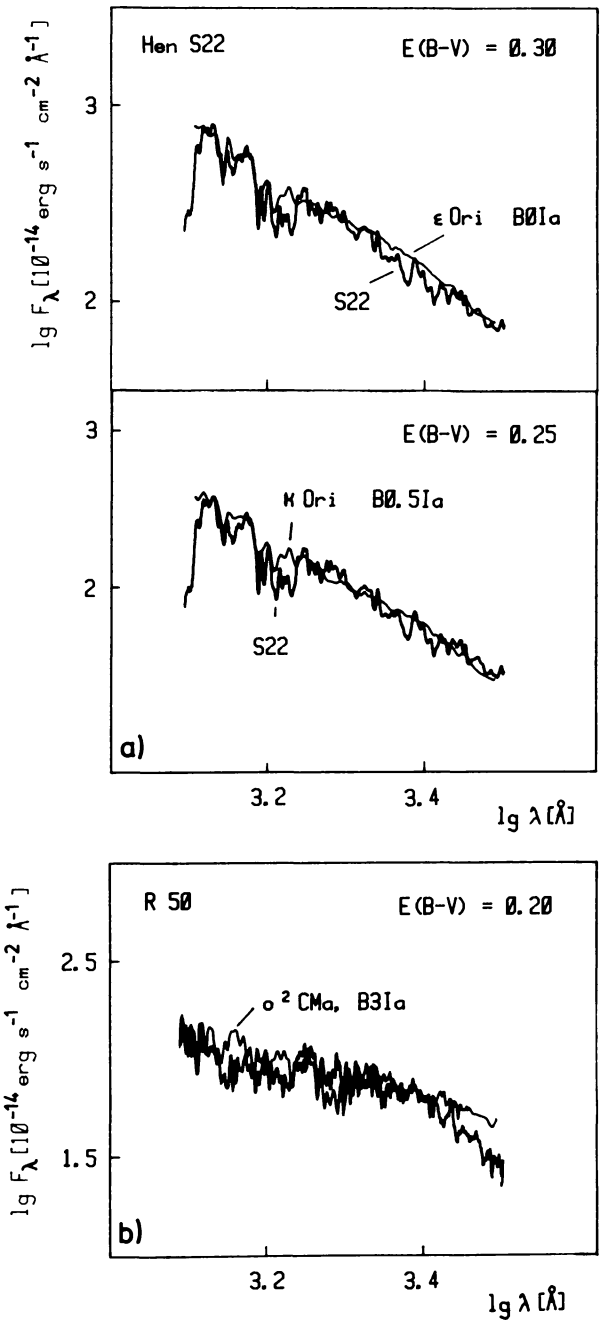

Fig. 12. a Comparison of the continuum energy distribution of Hen S 22 with two galactic supergiants of spectral types B0 and B0.5 for two values of $E(B-V)$. **b** Comparison of the continuum energy distributions of R 50 and a galactic B3Ia supergiant. The flux deficiency longward of 2300 Å ($\log\lambda = 3.4$) of R 50 can be explained by Balmer continuum absorption of cool circumstellar material

of the UV-line spectrum cf. Shore and Sanduleak (1984). They deduced a spectral type B0.5 from the equivalent widths of the absorption lines in the low resolution IUE spectrogram.

Although Hen S 12 is the object of our sample with the poorest observational material (one rather noisy coudé-spectrogram only) a hybrid character of the line spectrum is also obvious. The Doppler width of the Fe II- and [Fe II]-lines is much smaller ($v_D \approx 100\,\mathrm{km\,s^{-1}}$) than the maximum expansion velocity ($v_{max} = 550\,\mathrm{km\,s^{-1}}$) derived from the Balmer line absorption components. Wind velocities of this order are usually found from the Balmer lines in early B-type supergiants (cf. e.g. Sterken and Wolf, 1978), indicating the presence of a normal line driven stellar wind component in the B0.5 supergiant Hen S 12. Again the presence of pronounced Balmer line-P Cygni profiles may indicate that the object is seen under an intermediate inclination angle.

5.7. *R 4*

The spectrograms of this B[e]-supergiants are dominated by a very rich and complexe emission-line spectrum, including H, Fe II, Si II, Mg I, [O I], [Fe II], [S II], [N II], and [Fe III] lines. The Balmer lines have P Cyg profiles. In addition the star shows a conspicuous photospheric absorption spectrum (of spectral type B0Ia) and sharp "shell' absorption lines of Ti II and Cr II. Surprisingly these shell absorption features are redshifted with respect to the likely systemic velocity. Because of this and other complications a detailed evaluation of the complex spectrum of R 4 is given elsewhere (Zickgraf and Wolf, 1985). However, in spite of various peculiarities R 4 also shows large differences in the widths and velocities of "hot" and "cool" wind lines, which again argues for the presence of a two-component stellar wind. The Balmer line P Cyg profiles and the shell absorption features seem to indicate that R 4 and its wind are seen edge-on.

6. Evolutionary state and physical nature of the B[e]-supergiants

According to the spectroscopic and photometric results described and discussed above, the B[e]-stars of the MCs are (apart from R 66 which is of spectral type B8) luminous B0–B3 supergiants. Figure 15 shows the location of the eight B[e]-stars (together with the S Dor-variables of the LMC) in an HR diagram. As shown by the figure the B[e]-supergiants are located to the right of the main-sequence band. From a comparison with evolutionary tracks it is clear that they represent evolved evolutionary stages of massive ZAMS O stars. However, although their luminosities are comparable or only slightly lower than those of S Dor variables, the mass loss from the B[e]-supergiants appears to be much more stationary and stable.

As described in detail in Paper I the spectrum of R 126 can be explained by the assumption of a two-component mass loss, consisting of a "normal" radiation-driven wind (as observed in all hot high-luminosity stars) and an additional (slow) Be-star-type mass loss from the equatorial regions of the stellar atmosphere. As outlined above, all known B[e]-stars of the MCs can be explained by this hypothesis. The marked spectral differences observed between the individual B[e]-supergiants can be explained by assuming different (inclination) angles between the stars' equatorial planes and the line of sight. In this scenario the main difference between the (low luminosity) classical Be-stars and the B[e]-supergiants would be the strongly luminosity dependent (and therefore in the B[e]-supergiants strongly enhanced) radiation-driven hot polar wind.

Although the details of the (classical) Be-star phenomenon are not yet fully understood, it seems to be well established that in these stars rapid stellar rotation leads to an enhanced slow mass loss from the equatorial regions of their atmospheres. At first

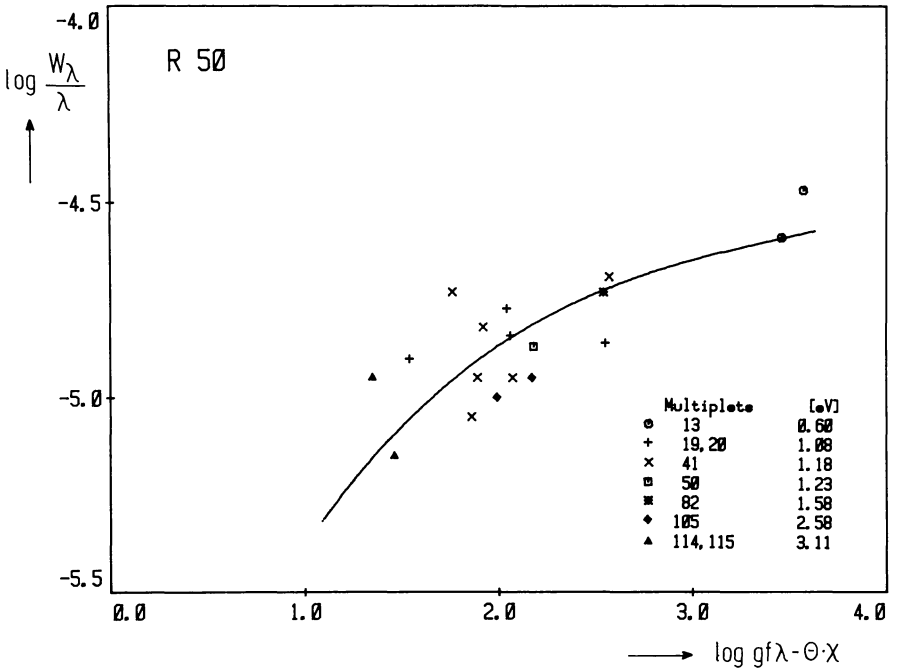

Fig. 13. Empirical curve-of-growth of the Ti II-absorption lines of R 50. The comparison with the theoretical curve-of-growth yields an excitation temperature of $T_{ex} = 10^4$ K

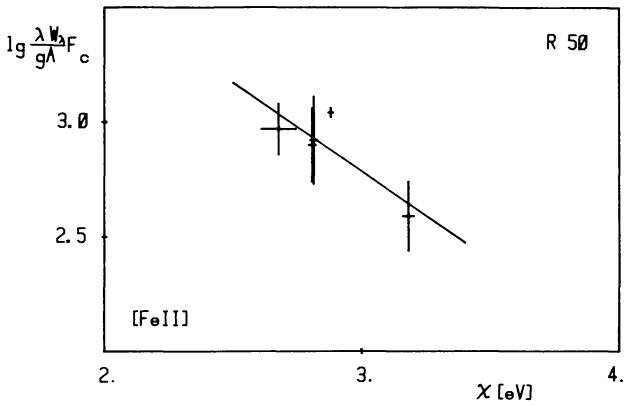

Fig. 14. Relative population numbers of the upper metastable levels of the [Fe II]-lines of R 50 plotted against their excitation energy. The gradient of the fitted line yields an excitation temperature of $T_{ex} = 6450$ K

glance, it appears unlikely that such rotational effects can play a role in supergiant stars as – for the case of local conservation of angular momentum – the ratio between centrifugal and gravitational acceleration at the surface decreases rapidly when the star evolves away from the main sequence. However, as shown by our observational data, the MC B[e]-supergiants are (together with the S Dor variables) in a region of the HR diagram where the combined opacities of many merging lines result in very small "effective accelerations" in the atmospheres, as the gravitational acceleration and the radiation pressure gradient (or "radiational acceleration") almost cancel each other (Appenzeller, 1985; Lamers, 1985). In such a situation even a centrifugal acceleration which is much smaller than the gravitational term can lead to a negative effective acceleration at the equator, which can be compensated only by an outward acceleration of matter, i.e. an enhanced mass loss. In addition, we note that due to convective angular momentum transport from the contracting innermost

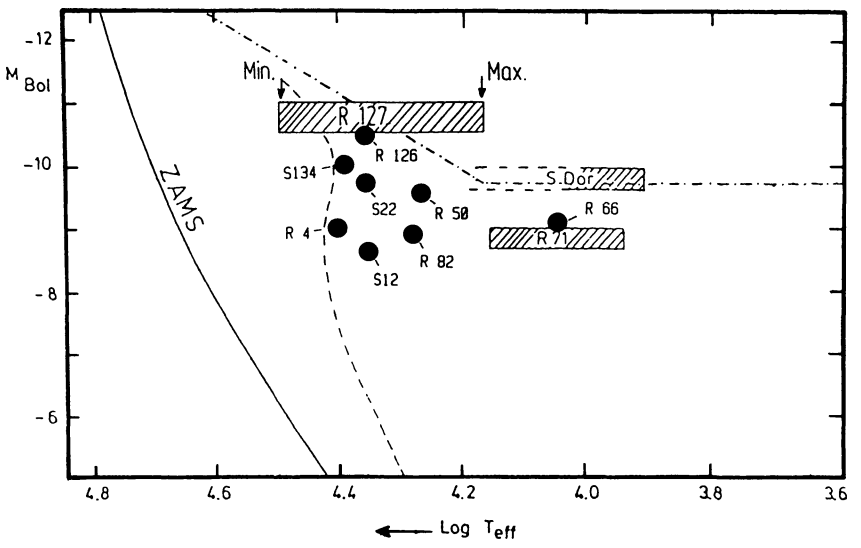

Fig. 15. HR-diagram showing the B[e]-supergiants and S Dor variables of the MCs. Also given are the boundaries of the main-sequence band (ZAMS = solid line, TAMS = broken line, according to Maeder, 1981). The dashdotted line indicates the upper limit of stellar luminosities (cf. Humphreys and Davidson, 1979).

layers and the loss of the outermost stellar layers in the main-sequence phase the rotation of the surface layers of very massive supergiant stars may be higher than expected from the local angular momentum conservation hypothesis. Unfortunately, our spectrograms do not allow to derive empirical surface rotation velocities of our program stars, since the measurable atmospheric line widths are dominated by other effects. Likewise, the internal angular momentum transport in stars and the details of the stellar winds of massive O stars are not accurately enough known for a safe prediction of the surface rotation. Therefore, we will have to wait for future observations or theoretical progress to reliably prove or disprove the two-component wind scenario outlined in Paper I and above for interpreting the complex properties of the B[e]-supergiants.

Acknowledgements. We are indebted to C. Sterken's "Long-Term Photometry of Variables" group who provided the Strömgren photometry of R 66. This work was supported by the Deutsche Forschungsgemeinschaft (SFB 132 and Wo 269, 2–1).

References

Allen, D.A., Glass, I.S.: 1976, *Astrophys. J.* **210**, 666
Appenzeller, I.: 1972, *Publ. Astron. Soc. Japan* **24**, 483
Appenzeller, I.: 1985, "Luminous Stars in Associations and Galaxies" (IAU Symp. 116), eds. C. de Loore and A. Willis.
Ardeberg, A., Brunet, J.-P., Maurice, E., Prevot, L.: 1972, *Astron. Astrophys. Suppl.* **6**, 249
Ardeberg, A., Maurice, E.: 1977, *Astron. Astrophys. Suppl.* **30**, 261
Azzopardi, M., Vigneau, J.: 1975, *Astron. Astrophys. Suppl.* **22**, 285
Basinski, J.M., Bok, B.J., Bok, P.F.: 1967, *Monthly Notices Roy. Astron. Soc.* **137**, 55
Bensammar, S., Friedjung, M., Muratorio, G., Viotti, R.: 1983, *Astron. Astrophys.* **126**, 427
Bessell, M.S.: 1979, *Publ. Astron. Soc. Pacific* **91**, 589
Butler, C.J.: 1972, *Dunsinck Obs. Publ.* **1**, 133
Cannon, A.J.: 1924, *Harvard Bull.* No. **801**
Caputo, F.: 1971: *Astrophys. Space Science* **10**, 93
Code, A.D., Meade, M.R.: 1979, *Astrophys. J. Suppl.* **29**, 195
Code, A.D., Davis, J., Bless, B.C., Brown, F.H.: 1976, *Astrophys. J.* **203**, 417
Dachs, J.: 1972, *Astron. Astrophys.* **18**, 271
Danks, A.: 1983, "The ESO User's Manual", Garching
Feast, M.W., Thackeray, A.D., Wesselink, A.J.: 1960, *Monthly Notices Roy. Astron. Soc.* **121**, 344
Friedjung, M., Muratorio, G.: 1980, *Astron. Astrophys.* **85**, 233
Garstang, R.H.: 1962, *Monthly Notices Roy. Astron. Soc.* **124**, 321
Glass, I.S.: 1977, *Monthly Notices Roy. Astron. Soc.* **178**, 9P
Glass, I.S.: 1984, *Monthly Notices Roy. Astron. Soc.* **209**, 759
Heck, A., Egret, D., Jaschek, M., Jaschek, C.: 1984, "IUE Low-Dispersion-Spectra Reference Atlas. Part 1", ESA SP-1052
Henize, K.G.: 1956, *Astrophys. J. Suppl.* **2**, 315
Humphreys, R.M., Davidson, K.: 1979, *Astrophys. J.* **232**, 409
Isserstedt, J.: 1978, *Astron. Astrophys. Suppl.* **33**, 193
Isserstedt, J.: 1979, *Astron. Astrophys. Suppl.* **38**, 239
Kurucz, R.L., Peytreman, E.: 1975, *Smithsonian Astrophys. Obs. Spec. Report* No. **362**
Lamers, H.J.G.L.M.: 1985, "Luminous Stars in Associations and Galaxies", (IAU Symp. 116) eds. C. de Loore and A. Willis.
Lucke, P.B., Hodge, P.W.: 1970, *Astron. J.* **75**, 171
Lucke, P.B.: 1974, *Astrophys. J. Suppl.* **28**, 73
Maeder, A.: 1981b, *Astron. Astrophys.* **102**, 401
Maurice, E.: 1976, *Astron. Astrophys.* **50**, 463
Mendoza, E.: 1970, *Bol. Obs. Tonantzintla Tacubaya* **5**, 269
Mihalas, D., Conti, P.S.: 1980, *Astrophys. J.* **235**, 515
Muratorio, G.: 1978, *Astron. Astrophys. Suppl.* **33**, 125
Muratorio, G.: 1981, *Astron. Astrophys. Suppl.* **43**, 111
Nandy, K., Morgan, D.N., Willis, A.J., Wilson, R., Gondhalekar, P.M.: 1981, *Monthly Notices Roy. Astron. Soc.* **196**, 955
D'Odorico, S., Enard, D., Lizon, J.L., Ljung, B., Nees, W., Ponz, D., Ratti, G., Tanne, J.F.: 1983, *The Messenger*, **33**, 1
Osmer, P.S.: 1973, *Astrophys. J.* **181**, 327
Ponz, D.: 1984, The MIDAS User's Guide, Chap. 12
Poeckert, R., Marlborough, J.M.: 1978, *Astrophys. J. Suppl.* **38**, 229
Rocca-Vollmerange, B., Prevot, L., Ferlet, R., Lequeux, J., Prevot-Burnichon, M.D.: 1981, *Astron. Astrophys.* **99**, L5
Schild, R.: 1976, in "Be and Shell Stars", IAU Symp. No. 70, ed. A. Slettebak (Reidel, Dordrecht), p. 107
Schmidt-Kaler, T.H.: 1982, in Landolt-Börnstein, New Series Group IV, Vol 2b, eds. K. Schaifers and H.H. Voigt, Springer, Berlin
Shore, N.S., Sanduleak, N.: 1983, *Astrophys. J.* **273**, 177
Shore, N.S., Sanduleak, N.: 1984, *Astrophys. J. Suppl.* **55**, 1
Smith, H.J.: 1957, *Publ. Astron. Soc. Pacific* **69**, 137
Stahl, O., Wolf, B., Zickgraf, F.-J., Bastian, U., de Groot, M.J.H., Leitherer, C.: 1983, *Astron. Astrophys.* **120**, 287
Stahl, O., Leitherer, C., Wolf, B., Zickgraf, F.-J.: 1984, *Astron. Astrophys.* **131**, L5
Stahl, O., Wolf, B., de Groot, M.J.H., Leitherer, C.: 1985, *Astron. Astrophys. Suppl.* **61**, 237
Sterken, C.: 1977, *Astron. Astrophys.* **57**, 361
Sterken, C.: 1983, ESO "*The Messenger*", No. **33**, 10
Sterken, C., Wolf, B.: 1978, *Astron. Astrophys.* **70**, 641
Struve, O., Wurm, K.: 1938, *Astrophys. J.* **88**, 84
Swings, J.-P.: 1973, *Astron. Astrophys.* **26**, 443
Thomas, J.A., Hyland, A.R., Robinson, G.: 1973, *Monthly Notices Roy. Astron. Soc.* **165**, 201
Unsöld, A.: 1955, Physik der Sternatmosphären, Springer Verlag, Berlin-Göttingen-Heidelberg, 2. Aufl., p. 416
Wamsteker, W.: 1981, *Astron. Astrophys.* **97**, 326
Westerlund, B.E.: 1961, *Uppsala Ann.* 5, No. **1**
Westerlund, B.E., Danziger, I.J., Graham, J.: 1963, *Observatory* **83**, 74
Wolf, B., Stahl, O., de Groot, M.J.H., Sterken, C.: 1981 *Astron. Astrophys.* **99**, 351
Zickgraf, F.-J., Wolf, B., Stahl, O., Leitherer, C., Klare, G.: 1985, *Astron. Astrophys.* **143**, 421
Zickgraf, F.-J., Wolf, B.: 1985, in preparation